Nuclear Inst. and Methods in Physics Research, A 883 (2018) 166–169

Contents lists available at ScienceDirect

Nuclear Inst. and Methods in Physics Research, A

journal homepage: www.elsevier.com/locate/nima

# Wave-optics modeling of the optical-transport line for passive optical stochastic cooling

M.B. Andorf [a,*], V.A. Lebedev [b], P. Piot [a,b], J. Ruan [b]

[a] Department of Physics and Northern Illinois Center for Accelerator & Detector Development, Northern Illinois University, DeKalb, IL 60115, USA
[b] Fermi National Accelerator Laboratory, Batavia, IL 60510, USA

ARTICLE INFO

*Keywords:*
Beam-cooling technique
Electron–laser interaction
Undulator radiation
Beam dynamics

ABSTRACT

Optical stochastic cooling (OSC) is expected to enable fast cooling of dense particle beams. Transition from microwave to optical frequencies enables an achievement of stochastic cooling rates which are orders of magnitude higher than ones achievable with the classical microwave based stochastic cooling systems. A subsystem critical to the OSC scheme is the focusing optics used to image radiation from the upstream "pickup" undulator to the downstream "kicker" undulator. In this paper, we present simulation results using wave-optics calculation carried out with the SYNCHROTRON RADIATION WORKSHOP (SRW). Our simulations are performed in support to a proof-of-principle experiment planned at the Integrable Optics Test Accelerator (IOTA) at Fermilab. The calculations provide an estimate of the energy kick received by a 100-MeV electron as it propagates in the kicker undulator and interacts with the electromagnetic pulse it radiated at an earlier time while traveling through the pickup undulator.

© 2017 Elsevier B.V. All rights reserved.

## 1. Introduction

The optical stochastic cooling (OSC) is similar to the microwave-stochastic cooling. It relies on a time dependent signal to carry information on the beam distribution and apply the corresponding cooling force [1,2]; see Fig. 1. In OSC a particle radiates an electromagnetic wave while passing through an undulator magnet [henceforth referred to as the pickup undulator (PU)]. The radiation pulse passes through a series of lenses and an optical amplifier and is imaged at the location of a downstream undulator magnet dubbed as kicker undulator (KU). The particle beam propagates through a bypass chicane ($B_1$, $B_2$, $B_3$, $B_4$) which provides an energy-dependent path length (i.e. time of flight) as well as a path length variation due betatron oscillations. The chicane also provides the space to house the optical components necessary for the optical-pulse manipulation and amplification. The imaged PU-radiation field and the particle that radiated it copropagate in the KU resulting in an energy exchange between them. When the time of arrival is properly selected a corrective energy kick is applied resulting in damping of the particles synchrotron oscillations as the process is repeated over many turns in a circular accelerator. If the KU is located in a dispersive section the corrective kick can also yield transverse cooling in the dispersive plane. Furthermore if the horizontal and vertical degrees of freedom are coupled outside of the cooling insertion the OSC can provide 6D phase-space particle cooling.

Although the nominal OSC scheme discussed in most of the literature involves an optical amplifier, the experiment planned in the 100-MeV IOTA electron ring at Fermilab [3,4] will not incorporate an optical amplifier in its first phase. This latter version of OSC is referred to as passive OSC (POSC) and it is considered throughout this paper. The nomination (amplified) OSC scheme will be implemented in a subsequent stage [5].

A comprehensive treatment of the OSC can be found in Ref. [6] where the kick amplitude is computed semi-analytically by considering a single focusing lens placed between the two undulators separated by a distance much larger than their length. In doing so the depth of field associated with the finite length of the undulators is suppressed. Although theoretically convenient, this focusing scheme is not practical and a three-lens configuration is instead adopted with focal lengths $f_i$ and distances $L_i$ fulfilling [6]

$$f_1 = L_2 \text{ and } \quad f_2 = -\frac{L_2^2}{2(L_1 - L_2)}, \tag{1}$$

where the parameters are defined in Fig. 1. The resulting transfer matrix between the KU and PU defined in the position-divergence coordinate

---

[*] Corresponding author.
*E-mail address:* mandorf1@niu.edu (M.B. Andorf).

https://doi.org/10.1016/j.nima.2017.11.094
Received 20 November 2017; Accepted 30 November 2017
Available online 6 December 2017
0168-9002/© 2017 Elsevier B.V. All rights reserved.

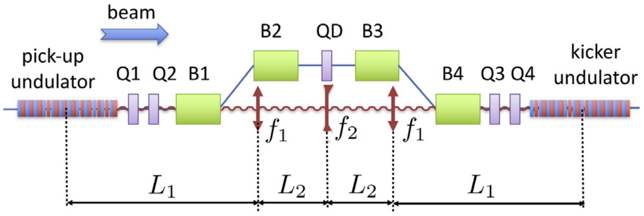

**Fig. 1.** Overview of the passive-OSC insertion beamline. The labels "$Q_i$", and "$B_i$" respectively refer to the quadrupole and dipole magnets and "$f_i$" represent the optical lenses. The solid blue (resp. ondulatory red) line gives the electron (resp. light) trajectory.

**Table 1**
Parameters for the optical telescope and undulators for the proposed POSC experiment at IOTA.

| Parameter, symbol | Value | Units |
|---|---|---|
| drift $L_1$ | 143 | cm |
| focal length $f_1$ | 143 | cm |
| drift $L_2$ | 32 | cm |
| focal length $f_2$ | −4.61 | cm |
| angular acceptance $\gamma\theta_m$ | 0.8 | |
| undulator parameter $K_u$ | 1.038 | |
| undulator length $L_u$ | 77.4 | cm |
| undulator period, $\lambda_u$ | 11.057 | cm |
| number of periods, $N_u$ | 7 | |
| on-axis wavelength, $\lambda_0$ | 2.2 | μm |
| electron Lorentz factor, $\gamma$ | 195.69 | |

system $\boldsymbol{X} = (x, x')$ is $M_{KU\to PU} = -I$, where $I$ is the $2 \times 2$ identity matrix. The three-lens telescope configuration supports a longitudinal point-to-point imaging between the PU and KU while also flipping the transverse coordinate w.r.t. the horizontal kicker axis. Correspondingly the telescope addresses the depth-of-field issue and the results derived for a single lens are directly applicable. The parameters of the optical telescope and undulators (the PU and KU are identical) are listed in Table 1. Note that both undulators are providing a vertical magnetic field $\boldsymbol{B} = B\hat{y}$ so that the oscillatory trajectory lies in the $(x, z)$ plane. The undulator radiation wavelength depends on the angle as: $\lambda_r = \frac{\lambda_u}{2\gamma^2}\left[1+\frac{K_u^2}{2}+(\gamma\theta)^2\right]$ where the parameters are defined in Table 1 and $\theta$ is the observation angle w.r.t the electron direction. Specifically, we defined the on-axis resonant wavelength as $\lambda_0 \equiv \lambda_r(\theta = 0)$.

## 2. Single-lens focusing

A wave-optics model of single-lens focusing was implemented in the Synchrotron Radiation Workshop (SRW) program [7,8] to benchmark our numerical implementation with the analytical model obtained for a single lens configuration [6].

Considering the case of POSC, taking $K_u \ll 1$, and assuming an infinite numerical aperture of the focusing lens, the on axis electric field amplitude imaged in the KU is given by

$$E_x(x = y = 0) = \frac{4}{3}eKk_u^2\gamma^3, \tag{2}$$

where $k_u \equiv 2\pi/\lambda_u$ ($\lambda_u$ is the undulator period) and $\gamma$ the Lorentz factor. The transverse velocity of the particle is $v_x = \frac{Kc}{\gamma}\sin(k_u z)$ and the kick amplitude is approximately

$$\Delta\mathcal{E} = e\int_0^{L_u}\frac{E_x K_u}{\gamma}\sin^2(k_u z)dz = \frac{eE_x K_u L_u}{2\gamma}, \tag{3}$$

where $L_u$ is the undulator length. Combining the latter equation with Eq. (2) yields

$$\Delta\mathcal{E} = \frac{2\pi}{3}(eK\gamma)^2 k_u N_u, \tag{4}$$

where $N_u$ is the number of undulator periods. Intuitively Eq. (4) is just equal to the total energy loss as the electron travels through one undulator. When $K_u$ is increased (thereby resulting in an increased angular deflection) and the finite angular acceptance of the lens, $\theta_m$, taken into account, the on-axis electric field $E_x(x = y = 0)$ in the KU is reduced by a factor $F_h(K_u, \gamma\theta_m) \leq 1$. The expression of $F_h(K_u, \gamma\theta_m)$ is derived in [6] and its dependence on $K_u$ appears in Fig. 2 for three cases of $\gamma\theta_m$. There is an additional efficiency factor, $F_u(\kappa_u) = J_0(\kappa_u) - J_1(\kappa_u)$, which accounts the effect of the longitudinal oscillation [given by $\frac{K_u^2}{8\gamma^2 k_u}\sin(2k_u z)$] of the particle in the KU where $\kappa_u \equiv K_u^2/4(1 + K_u^2/2)$. The kick amplitude from Eq. (4) is thus reduced by the factor of $F_h(K_u, \theta_m\gamma) \times F_u(\kappa_u)$.

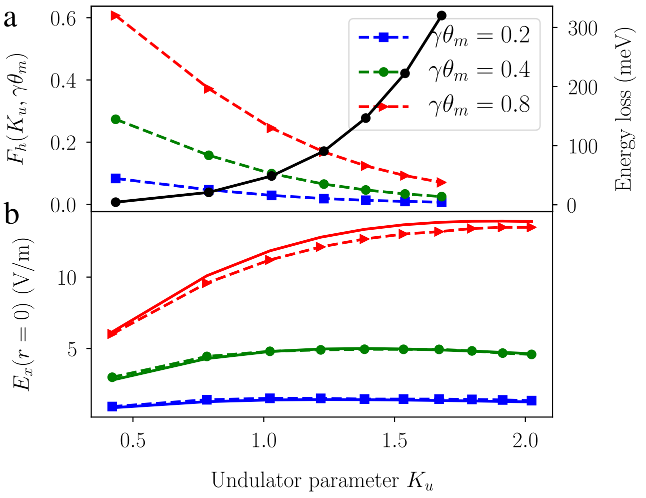

**Fig. 2.** Computed suppression factor $F_h(K_u, \gamma\theta_m)$ (dashed traces, left axis scale) and energy loss (solid traces) of the particle passing through one undulator (right axis scale) as a function of the undulator parameter $K_u$ for different angular acceptances of the lens ($\gamma\theta_m$) (a). Comparison of the electric field at the focus on a single lens analytically computed (solid traces) and simulated with SRW (symbol with dashed traces) for the same cases of angular acceptance (b).

The simulation in SRW are performed in the frequency domain: the field frequency components within the PU-radiation bandwidth are propagated and the field amplitude in the time domain inside the KU is computed [9]. This is first done for the case of a single focusing lens using $L_u$ and $\lambda_o$ from Table 1, but varying $N_u$ and other parameters appropriately. For this benchmarking simulation, the distance between the PU and KU centers is taken to be $L_t = 19.5$ m (i.e. $L_t \gg L_u$) in order to suppress the depth-of-field effect and the focal length of the lens is $f = L_t/2$. The simulated value for $E_x(K, \gamma\theta_m)$ are found to be in excellent agreement (relative difference below 5%) as shown in Fig. 2.

## 3. Imaging with a three-lens telescope

We now focus on the imaging scheme proposed for the POSC experiment at IOTA with parameters summarized in Table 1. The point-to-point imaging of the KU radiation in the PU is accomplished with a three-lens telescope. First, the field amplitude at the KU longitudinal center is compared with the expected value from theory: using Eq. (2) and $F_h(1.038, 0.8) = 0.25$ yields $E_x = 11.8$ V/m while SRW gives 10.9 V/m corresponding to a relative discrepancy < 7%. The kick amplitude using Eq. (4) and $F_u(0.18) = 0.91$ yields $\Delta\mathcal{E} = 22$ meV while directly computing the kick in the same way with SRW yields a value of 20.1 meV. Therefore the agreement between theoretical predictions and numerical simulations is reasonable as was already observed in the previous Section.

It should be noted that with SRW the longitudinal and transverse dependence of the electric field neglected in theory can also be accounted. The latter of which is from the effective aperture of the outer lenses being less at the edges of the undulator than they are at the center. To find the kick value from SRW, the time-domain field was computed

Download English Version:

https://daneshyari.com/en/article/8167005

Download Persian Version:

https://daneshyari.com/article/8167005

Daneshyari.com